Dragonfly M-C Graphs For Symbolic Analysis of Current-Conveyor Circuits

Dalibor Biolek
Dept. of EE & Dept. of Microelectronics
FEEC, Brno Univ. of Technology, & FVT, Univ. of Def.
Brno, Czech Republic
dalibor.biolek@unob.cz

Viera Biolkova and Zdenek Kolka
Dept. of Radio Electronics
FEEC, Brno Univ. of Technology
Brno, Czech Republic
{biolkova,kolka}@feec.vutbr.cz

***Abstract*—On the basis of the modified nodal analysis, universal matrices-stamps are defined for modeling several types of current conveyor. From these stamps, the so-called Dragonfly Mason-Coates' graphs are derived for a fast hand-and-paper symbolic analysis of current-conveyor circuits.**

Keywords-M-C graph; matrix-stamp; current conveyor

I. INTRODUCTION

Current conveyors belong to important components of modern blocks for analog signal processing [1]. Although the up-to-date analysis and simulation of electronic circuits are coupled with the utilization of computer programs, the hand-and-paper analysis of simple blocks still plays its useful role. The main reason is the necessity of having a symbolic formula for the verification of basic circuit functionality. In contrast to the SPICE-family programs for the numerical analysis, there are not many commonly available programs for symbolic analysis which would be able to analyze circuits with various types of today's active components [2]. Another reason for the hand-and-paper analysis is connected with the method of signal flow graphs, which can be used not only for the analysis but also as a supporting tool for the circuit synthesis.

Current conveyors (CCs) are elements whose presence in the circuit makes its intuitive analysis difficult. They have no admittance matrix. This fact complicates the inclusion of their models in the commonly used nodal analysis, and the modified nodal approach (MNA) must be used instead [3]. In the past, a number of attempts were made to find simple algorithms of compiling equations for circuits with CCs and other active components [3], particularly in the form of flow graphs [4], [5]. The common shortcoming of most approaches consists in the rather complicated rules of compiling a model of the circuit (i.e. flow graph) directly from the circuit schematics. Due to the transformation of circuit variables, caused by CC operation, the models of the conveyor and of the rest of the circuit blend together. This is in conflict with the basic advantage of the MNA, where every circuit element has its own description, which is modularly inserted into the pseudo-admittance matrix or into the oriented graph of the entire circuit. In addition, the transformation of circuit variables depends on the type of CC. That is why the method of building the circuit model is not universal. Owing to the transformation, the linkage to the circuit is not clearly evident from the flow graph, and such graphs are not appropriate for circuit synthesis and optimization.

This work has been supported by the Czech Science Foundation under grants 102/08/0784 and 102/09/1628, and by the research programmes of BUT No. MSM0021630503/513 and UD Brno No. MO FVT0000403, Czech Republic.

An additional disadvantage of the above approach in [4] consists in the absence of conveyor output current in the model equations. However, this current is a frequently required quantity, particularly for circuits operating in the current or the mixed modes.

In this paper, a "matrix-stamp" method of algorithmic analysis of circuits with CCs is shown which overcomes the above problems. We define a universal stamp, which can be used for all the basic types of CC. This matrix-stamp then leads to the so-called Dragonfly Mason-Coates' (M-C) graph [5] of CC with undirected self-loops. Three examples demonstrate the usefulness of these graphs for the analysis and synthesis of active filters.

II. MATRIX-STAMP AND M-C GRAPH-STAMP OF THÉVENIN MODEL OF RECIPROCAL ONE-PORT

Consider a circuit that is described by equations of Kirchhoff's current law (KCL) of the classical nodal analysis. The number of equations is equal to the number of independent nodes in the circuit. The equations contain the same number of unknown nodal voltages.

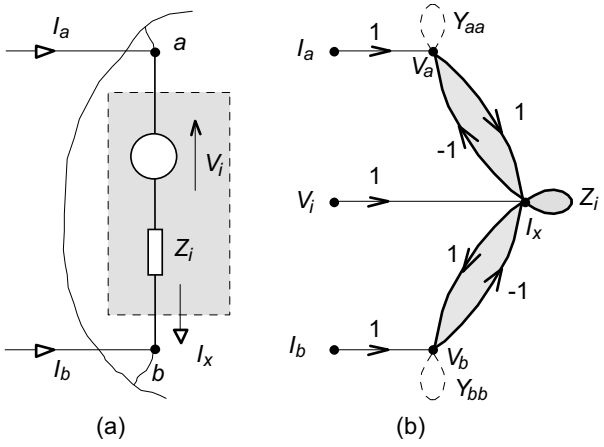

Figure 1. (a) Thévenin model of included one-port, (b) corresponding M-C graph-stamp.

$$Z_i I_x + V_b = V_i + V_a, \text{ or } V_i = Z_i I_x + V_b - V_a. \quad (1)$$

A one-port described by its Thévenin model according to Fig. 1 (a) is additionally connected between nodes *a* and *b* of the

978-1-4244-6815-7/10/$26.00 ©2010 IEEE

existing circuit. Then both the voltage and the current relations in the circuit will be changed. A current I_x will flow through the one-port and the current relations at nodes *a* and *b* will be violated. The original nodal voltages will also be changed.

The original equation describing the current equilibrium at node *a* should be completed by current I_x, flowing outside the node, and at node *b* by current I_x with negative sign because it flows into node *b*. In addition, nodal voltages V_a and V_b are now tied by the following condition:

All these modifications can be included in a new set of MNA equations:

			V_a	V_b		I_x	
a	I_a		Y_{aa}	…	…	+1	V_a
b	I_b		…	Y_{bb}	…	-1	V_b
	.	=	.	.	.	.	.
	.		.	.	.	.	.
	V_i		-1	1		Z_i	I_x

stamp

(2)

The vector of unknown nodal voltages is extended by another variable – current I_x. The number of equations is also increased by 1 by the above condition between nodal voltages V_a and V_b. The voltage V_i is included in the left-side vector of the known exciting quantities. The modification of KCL equations for nodes *a* and *b* is implemented by entering the numbers +1 and –1 into column „ I_x “.

The original circuit admittance matrix together with the stamp of the Thévenin model of the included one-port represents directions how to analyze – for instance – circuits with voltage sources by means of MNA. The impedance Z_i can be zero, which can model the ideal voltage source. For $V_i = 0$ and simultaneously $Z_i = 0$, we model a short connection between the nodes and the short-circuited current can be computed. This procedure can be used for the analysis of circuits with current-controlled sources.

The set of MNA equations (2) can be transformed into the form of (3) for a direct construction of the flow graph in Fig. 1 (b). See [5], [6] for more details about the M-C flow graphs.

$$\begin{aligned} Y_{aa}V_a &= I_a - I_x - \ldots \\ Y_{bb}V_b &= I_b + I_x - \ldots \\ &\ldots \\ Z_i I_x &= V_i + V_a - V_b \end{aligned} \qquad (3)$$

The symbol Y_{aa} (Y_{bb}) specifies the sum of admittances connected to node *a* (*b*). The corresponding undirected self-loops in the graph are drawn as dotted curves to show that the given admittances are not parts of the circuit in Fig. 1 (a).

The flow graph-stamp of the included two-port has a thick-line shape resembling the dragonfly. It is the graph representation of its matrix-stamp. New graph nodes are the input node V_i and the node of the unknown circuit variable I_x. Each “dragonfly wing” is formed by a couple of paths with gains of +1 and –1. The “outwards” directed paths are current paths (they are directed out of current node I_x). The path with the + sign follows the wing towards the node, to which the current I_x flows. The second path has the – sign. Voltage paths follow the opposite wing margins. They have both the directions and signs opposite to those of the current paths.

The “dragonfly head” is formed by a self-loop, the gain of which is given by the inner impedance of the Thévenin model. The “dragonfly tail” contains the node of inner voltage of the Thévenin model.

The above “dragonfly” model includes all existing models of reciprocal one-ports: for passive impedance, the “tail” will vanish. For the ideal voltage source the “head” gain will be zero. In the case of grounded one-port, only one “wing” will appear in the graph.

The dragonfly graph-stamp can be theoretically utilized in the analysis of circuits with both current and voltage sources. However, its practical importance appears when solving circuits with elements such as CCs, where current relations are under consideration.

In the case of nonreciprocal circuits – for instance OpAmps and all the types of CC – their flow graphs will contain “dragonflies” or similar structures after their transformations.

III. CIRCUITS WITH CCS

The symbol of the general three-port CC, which is included into a circuit at nodes *a*, *b* and *c*, is shown in Fig. 2 (a). This conveyor is described by general hybrid equations in the following form:

$$\begin{bmatrix} I_y \\ V_x \\ I_z \end{bmatrix} = \begin{bmatrix} & \alpha & \\ \beta & & \\ & \gamma & \end{bmatrix} \begin{bmatrix} V_y \\ I_x \\ V_z \end{bmatrix} \qquad (4)$$

TABLE I. COEFFICIENTS FOR VARIOUS TYPES OF CC.

coefficient	α	β	γ
CCI	1		
CCII	0		
CCIII	-1		
noninverting		1	
inverting		-1	
positive			1
negative			-1

The values of α, β, and γ coefficients depend on the type of CC as shown in Tab. 1. In addition, we can use them for modeling the basic conveyor inaccuracies. For example, deviating the value of the γ coefficient from 1 models the inaccuracy of the gain of internal current mirror of CCII+. Similarly, the deviation of β models the inaccuracy of voltage follower gain between the *x* and *y* inputs of a non-inverting CCII.

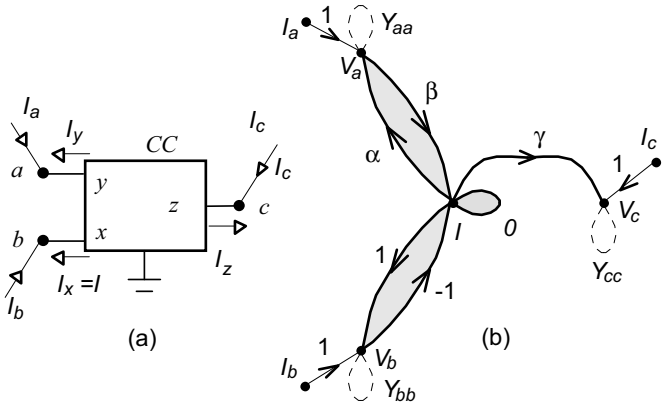

Figure 2. (a) three-port CC, (b) its dragonfly M-C graph.

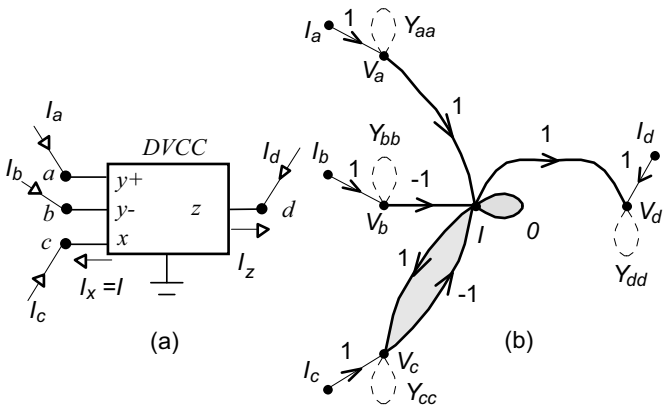

Figure 3. (a) Differential Voltage Current Conveyor (DVCC), (b) its dragonfly M-C graph.

The corresponding matrix-stamp can be derived from hybrid equations (4) and from Fig. 2 (a):

			V_a	V_b	V_c		I	
a	I_a		Y_{aa}	...	...	...	$-\alpha$	V_a
b	I_b		...	Y_{bb}	...	...	-1	V_b
c	I_c		...	...	Y_{cc}	...	$-\gamma$	V_c
	..	=	..	..	..	..	..	..
			β	-1				I

(5)

The symbol I indicates the independent current $I = I_x$.

The M-C graph of CC in Fig. 2 (b) is derived via a similar procedure as for the above Thévenin model. In comparison with the original "dragonfly" in Fig. 1 (b), the path gains on the upper wing are modified. One additional part models the current transfer into the CC output. The self-loop gain of node I is now 0. In the case of the well-known effect of nonzero resistance R_x of the CCII, this gain will be just R_x.

It should be noted that for the commonly used CCII type, the part with gain α disappears from the flow graph. This fact contributes to the graph simplification.

Figure 3 demonstrates the flexibility of the "dragonfly concept", which can also be applied to multi-port current conveyors. The well-known differential voltage CC in Fig. 3 (a) has high-impedance differential inputs y+ and y-. Due to this fact, the paths from I to V_a and V_b in Fig. 3 (b) are omitted. The equation $V_a - V_b - V_c = 0$ is modeled via the corresponding paths directed to the I node (the left side of the equation) and via the zero-gain undirected self-loop associated with the I node (the right side of the equation).

IV. Examples of Analysis

The 2nd -order high-input impedance insensitive filter in Fig. 4 (a) was published in [7]. Assume that the β and γ parameters of both CCII+ are not exactly equal to 1. Let us find the influence of these inaccuracies on the filter parameters.

To determine filter transfer function V_4/V_1, let us construct the shortened M-C graph in Fig. 4 (b), considering general parameters β_1, β_2, γ_1 and γ_2. The graph evaluation is considerably simplified owing to three zero-gain self-loops.

Applying the gain formula for M-C graphs [6] yields the result

$$\frac{V_4}{V_1} = \frac{\dfrac{\beta_1}{\beta_2}}{1 + \dfrac{R_4(C_1+C_3)}{\beta_2\gamma_1}s + \dfrac{R_2R_4C_1C_3}{\beta_2\gamma_1}s^2}, \qquad (6)$$

which is in accordance with [7]. The final formula enables a simple determination of the influence of β and γ coefficients on filter parameters ω_0 and Q.

As a second demonstration, a general impedance converter (GIC) with two CCs is given in Fig. 5 (a) [1]. As noted in [1], this circuit operates as a negative GIC, if both conveyors are of equal polarity, that is to say both are CCII+ or CCII-. On the contrary, if the conveyors are of opposite polarities, then a positive GIC is obtained. The prospective operation for other types of CC is not mentioned in [1].

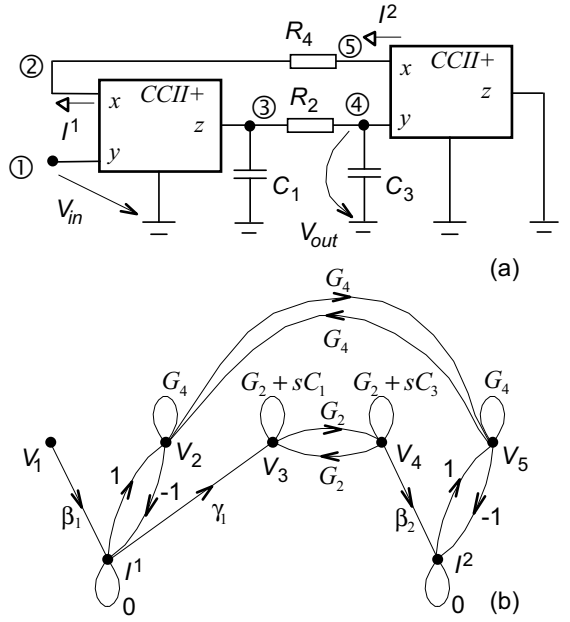

Figure 4. (a) 2nd -order filter [7], (b) its M-C graph.

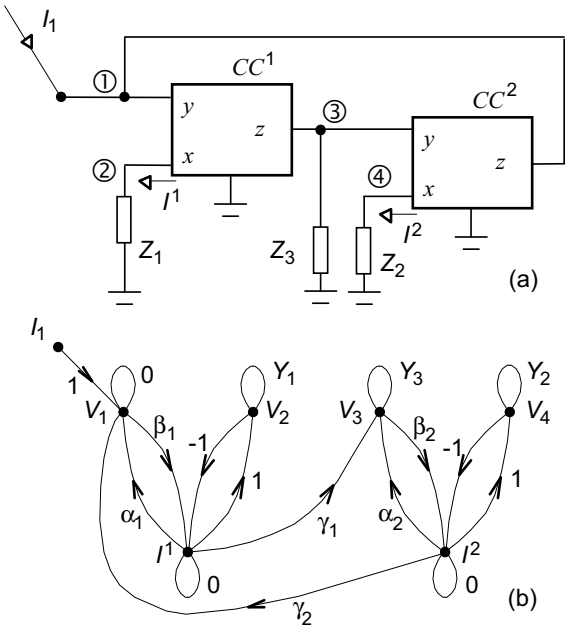

Figure 5. (a) GIC [1], (b) its M-C graph.

Consider the general CCs in Fig. 5 with their graphs-stamps according to Fig. 2 (b). The resulting M-C graph, constructed from the schematics, is shown in Fig. 5 (b). Evaluating it by inspection yields the formula for the input impedance:

$$Z_{in} = \frac{V_1}{I_1} = \frac{Y_3 - \alpha_2\beta_2 Y_2}{-\beta_1\gamma_1\beta_2\gamma_2 Y_1 Y_2 + \alpha_1\beta_1\alpha_2\beta_2 Y_1 Y_2 - \alpha_1\beta_1 Y_1 Y_3}. \quad (7)$$

After arrangement we have

$$Z_{in} = \frac{Y_3 - \alpha_2\beta_2 Y_2}{\beta_1 Y_1[\beta_2 Y_2(\alpha_1\alpha_2 - \gamma_1\gamma_2) - \alpha_1 Y_3]}. \quad (8)$$

Utilizing two CCIIs, we set $\alpha_1 = \alpha_2 = 0$. Then Eq. (8) yields:

$$Z_{in} = -\frac{1}{\beta_1\gamma_1\beta_2\gamma_2}\frac{Z_1 Z_2}{Z_3}. \quad (9)$$

This result confirms the above conclusions from [1] and extends them to the possibility of utilizing both the classical and the inverting CCs (for inverting CCs, coefficients β are negative).

Analysing Eq. (8), we conclude that both conveyors must be of the CCII type to achieve the simple impedance conversion according to Eq. (9).

Figure 6 (a) shows a DVCC-based all-pass filter from [8]. Since the *y*- and *x* terminals are interconnected, the gain of the path from node V_x to node I_{out} is -2. For *x*-terminal resistance $R_x = 0$, the graph evaluation is easy:

$$\frac{I_{out}}{I_{in}} = \frac{G_1 + sC - 2sC}{0 - sC - (sC)^2.0 + 2(G_2 + sC)} = \frac{1 - sCR_1}{2R_1/R_2 + sCR_1}.$$

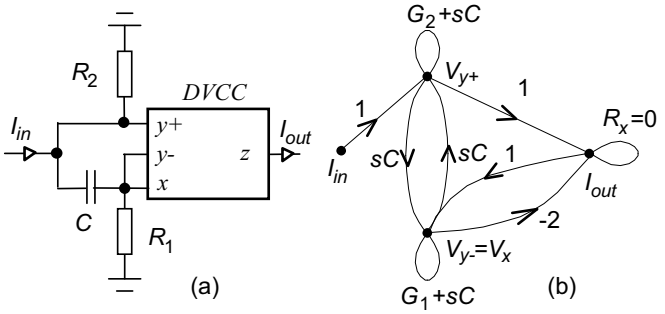

Figure 6. (a) All-pass filter [8], (b) its M-C graph.

This result confirms the all-pass character of this circuit for $R_2 = 2R_1$ [8].

Taking nonzero parasitic resistance R_x into account, the graph evaluation yields a more precise condition $R_2 = 2R_1/(1+R_x/R_1)$, indicating also the DC gain modification to the value $R_2/(2R_1+R_x)$.

V. CONCLUSIONS

Novel modified M-C graphs are described in the paper. They enable a simple modeling of current conveyors CCI, CCII, and CCIII regardless of whether they are positive, negative, non-inverting or inverting. Selecting the values of α, β, and γ coefficients and the self-loop gain of current node in the graph, we can also model some basic CC non-idealities such as the inaccuracy of the internal voltage follower between terminals *y* and *x*, the influence of nonzero resistance R_x, inaccuracies of internal current mirror, etc., without any modification of the flow graph topology. An extension of this approach to multi-port conveyors is also shown on an example of the differential voltage current conveyor (DVCC).

REFERENCES

[1] C. Toumazou, Circuits & Systems. Tutorials. ISCAS'94, London, 1994, p. 580.

[2] Z. Kolka, D. Biolek and V. Biolkova, "Symbolic Analysis of Linear Circuits with Modern Active Elements," WSEAS Trans. on Electronics, vol. 5, no. 6, pp. 88-96, 2008.

[3] M. Fakhfakh et al, Design of analog circuits through symbolic analysis. Bentham Science Publishers Ltd., 2010.

[4] D. Biolek, "Novel signal flow graphs of current conveyors," 38th MWSCAS, Rio de Janeiro, Brazil August 13-16, 1995, pp. 1058-1061.

[5] D. Biolek and V. Biolkova, "Flow graphs suitable for teaching circuit analysis," Applications of Electrical Engineering (AEE'05), Prague, Czech Republic March 13-14, 2005, pp. 33-35.

[6] D. Biolek, Solving Electronic Circuits. BEN, Prague, Czech Republic, 2004.

[7] A. Fabre et al, "High Input Impedance Insensitive Second-Order Filters Implemented from CCs," IEEE Trans. CAS-I, vol. 41, no. 12, pp. 918-921, 1994.

[8] S. Minaei, M.A. Ibrahim and H. Kuntman, "DVCC based current-mode first-order all-pass filter and its application," 10th IEEE Int. Conf. on Electronics, Circuits and Systems (ICECS), 2003, pp. 276-279.